Radiative electron capture by oxygen ions in single-crystal channels: Experiment and theory

B. R. Appleton, R. H. Ritchie, J. A. Biggerstaff, T. S. Noggle, S. Datz, C. D. Moak, H. Verbeek,* and V. N. Neelavathi†
Oak Ridge National Laboratory, Oak Ridge, Tennessee 37830
(Received 6 November 1978)

The phenomenon of radiative electron capture (REC) has been studied for 17–40-MeV O ions channeled through thin single crystals of Ag and Si. As a consequence of the unique constraints imposed on the interactions of well-channeled ions, it is possible to study the REC phenomenon for fully stripped oxygen ions interacting primarily with the free or weakly bound electrons in single-crystal channels. Radiation is identified which results from electrons captured directly into the lowest-energy state of the moving oxygen ions as well as that arising from a number of bremsstrahlung processes. The measured cross sections and widths of the REC radiation and the bremsstrahlung processes are compared to calculations made specifically for the channeling situation. The calculations incorporate standard radiation theory and a statistical model of the electron states in the single crystal. The space-varying electron density is averaged over impact parameters appropriate for the channeled ions. The measured REC cross sections show a marked deviation from theory which is not understood at this time. The shapes of the REC lines and the x-ray background present in the measured spectra are in reasonable agreement with the calculations, but the widths of the REC lines as a function of ion energy show only fair agreement. Results of these studies are discussed and possible explanations offered for some of the discrepancies.

I. INTRODUCTION

The phenomenon of radiative electron capture (REC), whereby an ion captures an electron into one of its shells and emits a photon, has been known for some time from studies in astrophysics and in the physics of laboratory plasmas. Similarly the theoretical description of this process by Bethe and Salpeter is well known.[1] The first observation of REC by energetic heavy ions in solids was reported only recently, however, by Schnopper *et al.*[2] Since then numerous experimental studies in solid and gaseous targets and theoretical investigations have been initiated in this area, resulting in a significant increase in the understanding of phenomena associated with the generation of photons by swift ions.[1–11] One of the most promising aspects of the REC phenomena which was noted by Schnopper *et al.*[2] in their original paper was the possibility that the widths of the REC lines could be interpreted to give information about the velocity distributions of electrons captured from the solid. Practical complications, however, arising as a result of normal ion-solid interaction phenomena, make such information difficult to extract. It was, in fact, the solid-state aspects of the REC effect which prompted our initial investigations[6] of which the work described below is an extension.

The experimental approach taken here has several advantages for studying the REC effect in solids. It exploits the unique constraints imposed on the interaction of a channeled heavy ion with the solid in which it moves. As we shall see, the channeling environment makes it possible to study the REC effect for a fully stripped ion, of primarily one charge state, interacting with a nearly free (valence-electron) gas. This provides unique insights into the REC phenomenon itself and, once the experimental techniques are perfected, the velocity distributions for particular single-crystal orientations will be more amenable to interpretation than those appropriate to polycrystalline solids. This channeling technique also provides well-defined boundary conditions for a theoretical analysis of the effect which is developed and presented in this paper.

II. EXPERIMENTAL TECHNIQUE

A. Experimental apparatus

The experimental arrangement is shown schematically in Fig. 1. Oxygen ion beams obtained from a Tandem Van de Graaff accelerator were energy selected, passed through a thin carbon-stripper foil, charge selected in an analyzing magnet, collimated to an angular divergence $\leq 0.05°$ full width, and directed onto a thin single crystal held in a three-axis goniometer. Thin self-supporting single crystals of Ag and Si (see Ref. 12) were oriented relative to the incident ion beams with an accuracy of 0.01° using

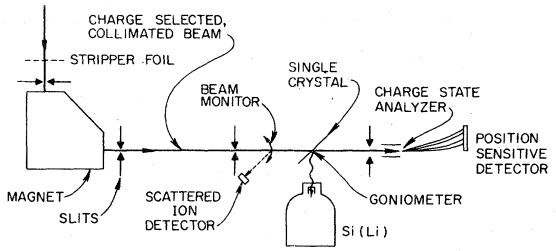

FIG. 1. Schematic diagram of experimental arrangement.

the goniometer. Oxygen ions transmitted through the crystal were charge and energy analyzed, using either an electrostatic analyzed (as shown) or a high-resolution magnetic spectrometer. Channeling measurements of the transmitted energy distributions of each emerging charge state as a function of crystal orientation were obtained in this way. Emergent charge-state distributions were also determined. Measurements of the photon spectra excited by the ions were recorded using Si(Li) detectors with an active area of 25 mm^2 and positioned at 90° to the incident beam direction, 5.5 cm directly below the point where the beam intersected the crystal. The Si(Li) detectors used were isolated in their own vacuum by either a 0.0003-in. or 0.0005-in Be window with resolution of 190 or 200 eV, respectively for 5.9-keV x rays. A calibrated beam monitor was used to obtain relative yield measurements.

B. Channeling effect

The phenomena associated with channeling of energetic positive ions in single crystals have been studied for many years and are well understood in most instances.[13] A well-collimated beam of ions directed parallel to a low-index direction in a single crystal encounters symmetrically arranged rows or planes of atoms and, consequently, the ions undergo sequential collisions with the lattice atoms in which the impact parameters are correlated. The result is that the vast majority of the incident ions acquire oscillatory trajectories in the open regions (channels) between the rows or planes of atoms. The main consequence of channeling is that it imposes unique constraints on the interactions of the channeled ions in contrast to the interactions of ions traveling in a polycrystalline or amorphous solid, or in a random direction in a single crystal. A number of channeling effects that are relevant to the present investigations for oxygen ions have been studied extensively[6,10,13–19] and form the basis for the experimental technique reported in this work.[6,10] The behavior of 10–40-MeV O ions transmitted parallel to the low-index planar and axial directions of thin Au and Ag single crystals are well understood on the basis of channeling models which have been used to: (i) deduce the parameters of the interaction potential between the channeled ions and atoms of the solid,[14,15] (ii) relate the stopping power of channeled ions to the ion trajectory and random stopping power,[14,15] (iii) determine the charge-changing cross sections of channeled versus randomly directed ions,[16–18] (iv) determine the effects of dynamic screening and ionic charge state on the stopping power of fully and partially stripped, channeled oxygen ions,[18] and (v) characterize completely the axial channeling behavior of oxygen ions as a function of incident charge states.[19]

The important consequences of these studies for the present investigation are that more than 95% of the oxygen ions are channeled along the major axial directions ([001] and [011]) and never approach closer than $\sim 10^{-9}$ cm to atoms on normal lattice sites, thereby eliminating interactions such as characteristic x-ray excitation which require close impacts ($\sim 10^{-12}$ cm). Because of the channeling effect[6,16–18] oxygen ions incident with charge states 8+ (fully stripped), 7+, and 6+ are virtually unable to capture electrons in a channel. This can be seen from the measured charge distributions for 27.8- and 40-MeV oxygen ions shown in Fig. 2.[18] When O^{8+}, O^{7+}, or O^{6+} ions are incident in a random direction of the thin Ag single crystal, the emerging ions have an equilibrium charge-state distribution independent of input charge states (dashed curves). However, when incident in a channeling direction ([011] axis) the emerging channeled ions are predominantly fully stripped (O^{8+}), are not at equilibrium, and have some memory of incident charge state.

Very recent measurements suggest that much of electron capture that is measured for channeled ions actually occurs in the several monolayers of surface contamination present on the entrance and exit surfaces of the thin single crystals. The results from such measurements are summarized in Fig. 3 for 27.5-MeV O ions transmitted parallel to the (111) planes of a 0.54-μm Ag single crystal. Previous investigations have shown that the stopping power of an energetic oxygen ion in a single-crystal channel is proportional to the square of the charge state of the ion, i.e., that $S_e \alpha Z_1^2$.[18] As examples, the two uppermost spectra in Fig. 3 show the transmitted energy spectra measured in a high-resolution magnet for O^{8+} and O^{7+} ions emerging when O^{8+} and O^{7+} ions, respectively, were incident parallel to (111). This correlation of input and exit charge state assures that the ion has not changed charge during its transmission through the channel. The two spectra peak at separate emergent energies, marked on Fig. 3 by the dashed lines which correspond to stopping powers in the ratio $S(8+)/S(7+) = 8^2/7^2$. Having established that the charge state of an ion inside the crystal can be deduced from its measured stopping power, en-

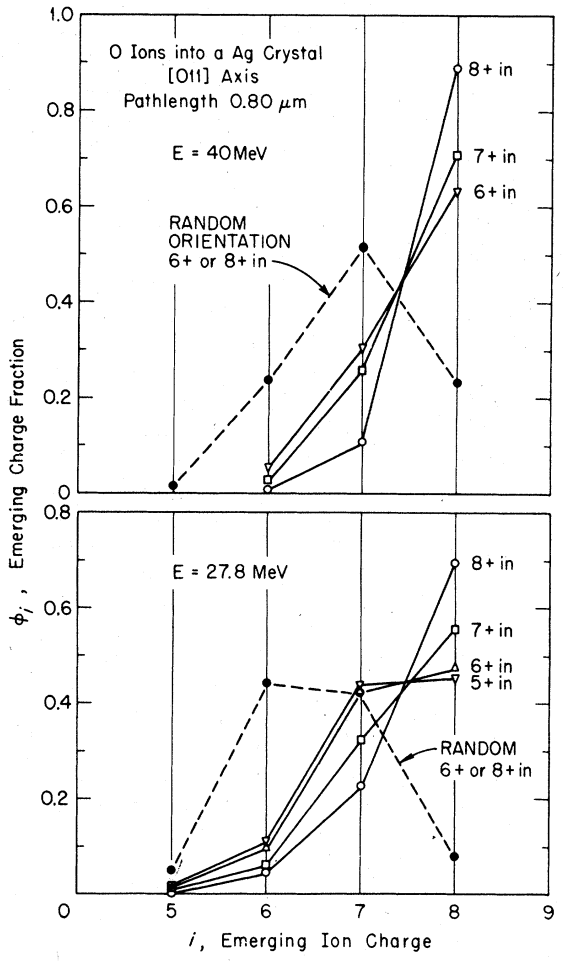

FIG. 2. Measured emergent charge-state distributions for oxygen ions transmitted in a random direction and parallel to the [011] axial channels of a 0.8-μm Ag single crystal.

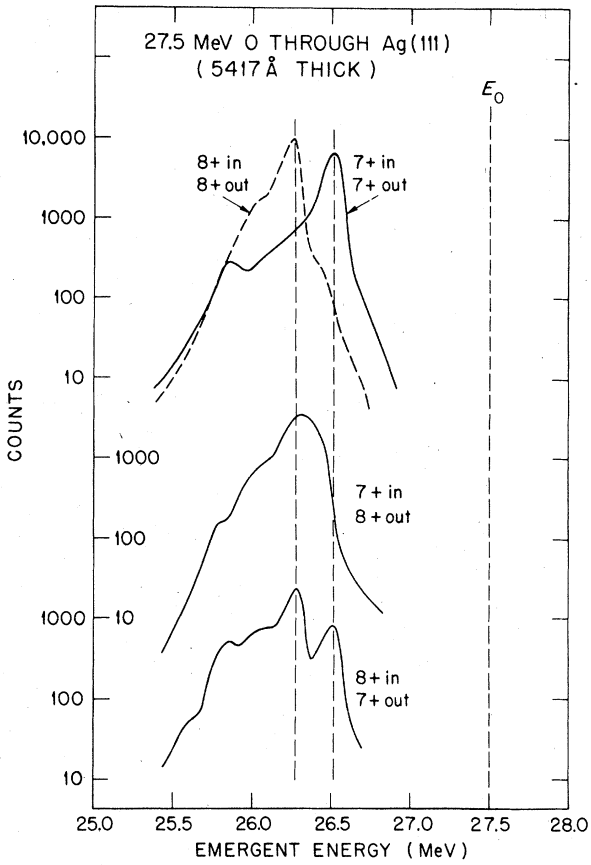

FIG. 3. Emergent energy distributions measured for 7+ and 8+ oxygen ions transmitted parallel to the (111) channels of a thin Ag single crystal.

ables us to draw some interesting conclusions concerning charge exchange in the crystal from the two remaining spectra. When O^{7+} is injected and the energy spectrum of emerging O^{8+} ions is measured (middle spectrum) one sees a continuous distribution in energy from the 8+ to 7+ peak energies, indicating that the ions changed from 8+ to 7+ throughout the thickness of the crystal by electron capture. However, when O^{8+} is injected and the emerging O^{7+} distribution is measured, two distinct peaks are present in the transmitted energy spectra centered on the energies of the 8+ and 7+ peaks (bottom spectra). This implies that the O^{8+} ions either captured an electron at the entrance surface of the crystal and remained 7+ throughout, or entered and remained O^{8+} until the exit surface where an electron was captured. These Ag crystals are known to have typically one to three monolayers of oxygen, sulfur, or carbon surface contamination as determined from Auger and ion scattering analysis. This means that nonradiative electron capture of electrons in these surface layers may account for a substantial portion of the charge-changing cross sections determined for single-crystal channels[16–18] ($\sim 10^{-19}$ cm^2), and that, in fact, a substantial fraction of electron capture which actually occurs in the free-electron environment of the channel is radiative electron capture. Whether this speculation is true or not, Fig. 3 is strong evidence for a surface capture mechanism of some sort.

C. Radiative electron capture (REC) and bremsstrahlung

A wealth of phenomena contribute to the x-ray distributions observed when solids are bombarded with energetic heavy-ion beams.[20–22] The collision system for a projectile ion of mass M_1, atomic number A, and incident energy E, bombarding a solid target (M_2,Z_2) is shown schematically in Fig. 4 as viewed

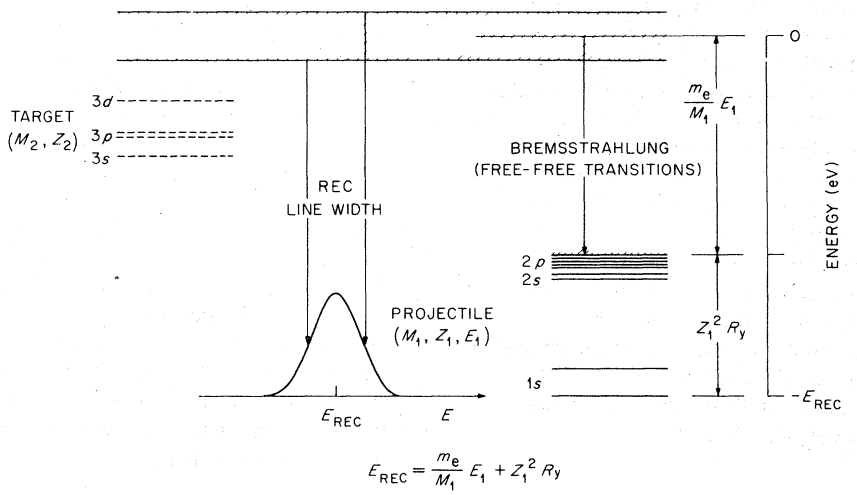

FIG. 4. Schematic representation of the radiative electron-capture effect viewed from the rest frame of the projectile ion.

from the rest frame of the projectile ion. Contributing effects observable for 10–40-MeV O ions bombarding Ag and Si are:

1. *Target characteristic x rays*

Incident O ions eject inner-shell electrons from target atoms and these vacancies are filled by outer-shell electrons with the energy gained in the transition radiated as an x-ray photon. In the present measurements Ag L x rays are most prominent. One should be aware that numerous complications affect the understanding of x rays excited by heavy ions: the charge states of heavy-ion projectiles affect the magnitude of the x-ray emission cross sections[23] and fluorescence yields[24]; the strong ionizing effects shift the energies of the characteristic x rays[20–25]; molecular orbital x-ray excitation mechanisms[20,21] can greatly increase x-ray emission cross sections and contribute continuua background[26]; and a host of "solid-state" effects exist for heavy-ion bombardment of solid targets.[27]

2. *Projectile characteristic x rays*

If the incident oxygen ion carries electrons into a collision where it becomes excited, or if it captures an electron from the solid into an outer shell and then decays, characteristic oxygen x rays can result. In Fig. 4, the maximum energy for such x rays can be seen to be Z_1^2 Ry, which is the series limit corresponding to a transition from the continuum of a totally ionized oxygen ion into the K shell. (Ry is the Rydberg unit, Ry = 13.6 eV.)

3. *Beschleunigungsstrahlung*

This process, the emission of "acceleration radiation," results when target electrons are accelerated by the Coulomb field of the incident nucleus. For a fixed projectile velocity the cross section is proportional to Z_1^2, and the major contributions to the cross section occur at distances the order of the Compton wavelength or shorter ($\hbar/m_e c = 3.85 \times 10^{-11}$ cm and where m_e is the electron mass).[28] However, since this distance is smaller than the average radius of the O K shell,[29] the beschleunigungsstrahlung yield is not expected to depend strongly on the charge state of the incident ion, although this could be investigated in channeling experiments. The photon distribution should decrease rapidly with increasing photon energy and have a high-energy cutoff at $\approx(m_e/M_1)E_1$. One can see from Fig. 4 that this corresponds to a free-free transition in which an electron from the solid is captured into the continuum of the moving oxygen ion. Recent observations of such radiation from strongly bound electrons[3,4] have been reported. The channeling technique reported here could easily be applied to study this emission for both strongly bound and free (conduction) electrons. Note that beschleunigungsstrahlung has been termed inverse bremsstrahlung.[3,4] However, the latter term is used in plasma physics to describe a different physical phenomenon, viz., the absorption of a photon by a nearly free electron which scatters on an ion in the absorption process.

4. *Secondary-electron bremsstrahlung*

Secondary electrons are produced with high probability by the incident oxygen ions and can emit a

bremsstrahlung quantum by being accelerated in the nuclear field of a target atom during the slowing-down process. The kinetic energy distribution of the knock-on electrons varies as $1/T^2$ with transferred energies T, up to a maximum of $T=4(m_e/M_1)E_1$ for free electrons (slightly higher energies are possible for strongly bound electrons). The resultant bremsstrahlung energy dependence is nearly the same, decreasing rapidly for photon energies above $4(m_e/M_1)E_1$. Secondary-electron bremsstrahlung for nonchanneling situations have also been reported previously.[22,30] Although secondary-electron bremsstrahlung is most important for thick targets, it can also contribute significantly for targets as thin as those used here (3000–7000 Å) especially when bombarded with heavy-ion beams.

5. *Projectile bremsstrahlung*

Bremsstrahlung resulting from collisions between the incident ions and target atoms is greatly suppressed compared to electron bremsstrahlung because the cross section depends inversely on the mass of the ion. Furthermore, channeled ions do not approach close enough to target atoms to emit appreciable bremsstrahlung. The photon continuum from this process would have a high-energy cutoff of $\approx E_1$.

6. *Radiative electron capture (REC)*

Capture of a target electron by a highly-stripped projectile ion can proceed either radiatively or nonradiatively. Normally, nonradiative electron capture is the dominant mechanism, but two important constraints imposed on channeled heavy ions, tends to make the radiative process relatively more important than in the random case.

(a) Since channeled ions never approach closer than $\sim 10^{-9}$ cm to atoms on normal lattice sites, their probability of capturing bound electrons is reduced over that for ions interacting in a random fashion with the atoms of a solid. This tends to suppress nonradiative capture and certainly contributes in part to the greatly reduced-charge exchange cross sections observed for channeled ions. Capture of valence electrons can occur through Auger processes, however.

(b) Although the cross sections for radiative capture are, in general, smaller than those for nonradiative capture because of the smallness of the coupling of the electron with the electromagnetic field, the REC process can proceed by capture of free, as well as bound electrons, since the photon emission allows for energy and momentum conservation. Furthermore, channeled ions interact freely with the weakly bound or conduction electrons by virtue of their trajectories in the single crystal. At sufficiently high-ion velocities radiative charge transfer can become the dominant mechanism even for bound electrons.[11]

The energetics of the REC process are depicted schematically in Fig. 4. Fully stripped ions (M_1,Z_1) with incident energy E_1, which capture electrons from the conduction band of the metal target (M_2,Z_2), will give rise to a photon line centered at an energy $E_{\mathrm{REC}}=(m_e/M_1)E_1+Z_1^2$ Ry. The width of the line is determined by the momentum distribution of the captured conduction electrons. As we shall see, the channeling technique offers not only the possibility of studying the REC process itself but of obtaining information about the solid-state aspects of the target. It was this latter prospect which prompted our initial investigations in this area.[6]

III. MEASUREMENTS

A. Basis of channeling measurements

As we have discussed, the basis of the experimental technique derives from the restricted interactions experienced by channeled heavy ions. The consequences of the channeling effect are illustrated in Fig. 5, which contrasts the observed photon spectra for 27.78-MeV O^{7+} ions incident parallel to the [011] axial channels, and along a random orientation of a 0.62-μm Ag single crystal. When the single crystal is purposely misoriented so that the ions encounter the lattice atoms at random as they would in an amorphous or polycrystalline Ag sample, one obtains the spectrum labeled random (solid circles) in Fig. 5. The prominant features above 2.5 keV are characteristic Ag L x rays excited by the incident oxygen ions. When the beam is channeled along the [011] (open circles, Fig. 5) the yield of Ag L x rays is reduced to $\approx$3% of that observed for the random orientation, i.e., only those ions *not* channeled, the so-called minimum yield fraction, excite Ag L x rays. The two spectra in Fig. 5 have been normalized by the minimum yield fraction for comparison purposes and have also been corrected for estimated x-ray absorption effects in the beryllium window, and the Si(Li) detector Au contact and dead layer. The effect of the normalization is to make the Ag L-x-ray peaks coincident, as expected. The most striking difference between the two spectra, however, is the prominent peak evident in the channeling spectrum between 1.5 and 2.0 keV. This peak results from radiative electron capture of target conduction electrons. As we shall see later, the energy of the peak is consistent with capture of a free electron by a fully stripped O ion into its innermost shell and the width of the peak, which is determined by the velocity distribution of the electrons in the [011] channel which are cap-

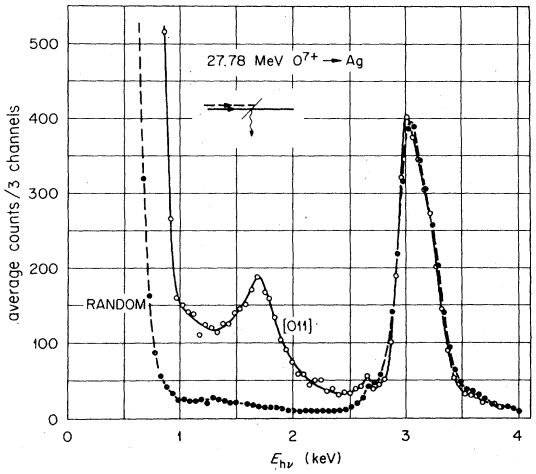

FIG. 5. Normalized photon spectra measured for 27.78-MeV O^{7+} ions transmitted parallel to the [011] and in a random direction of a 0.62-μm Ag single crystal.

tured, shows reasonable agreement with expectations.

There are several advantages of the present technique for studying REC in single-crystal channels as opposed to studying REC in polycrystalline targets:

(i) Channeled O ions are predominantly of one charge state for the reasons discussed earlier. In contrast, heavy ions incident in polycrystalline targets have a distribution of charge states,[7] and the energies and widths of the REC photons for the different charge states will interfere and complicate interpretation. This can be illustrated by taking a closer look at the random spectrum of Fig. 5, which is reported on an expanded scale in Fig. 6. Close scrutiny shows evidence of a poorly resolved broad peak at about 1.3 keV, which is likely due to REC to various oxygen charge states.

(ii) The channeling effect greatly reduces close encounters between the ions and bound target electrons without diminishing the ion interactions with the free or conduction electrons. This renders the REC of free electrons a much more prominent feature relative to the characteristic target x-ray background (as Fig. 5 clearly shows) and thus more amenable to direct investigation.

(iii) In the channeling configuration most of the incident ions appear to be in a single charge state interacting primarily with conduction electrons. This imposes well defined boundary conditions on the REC effect which should be more amenable to theoretical calculations (i.e., a hydrogen-like ion in a free electron gas).

(iv) The channeling environment as viewed from the rest frame of, say, a 40-MeV O^{8+} ion, is the experimental analogue of a fully stripped oxygen ion being bombarded by an electron gas having a density the order of 10^{22} to 10^{23} electrons/cm^3 and moving with kinetic energy $\sim$1.4 keV. This situation may sufficiently approximate the interactions experienced by an impurity ion in a dense controlled thermonuclear-reactor-type plasma to make the chan-

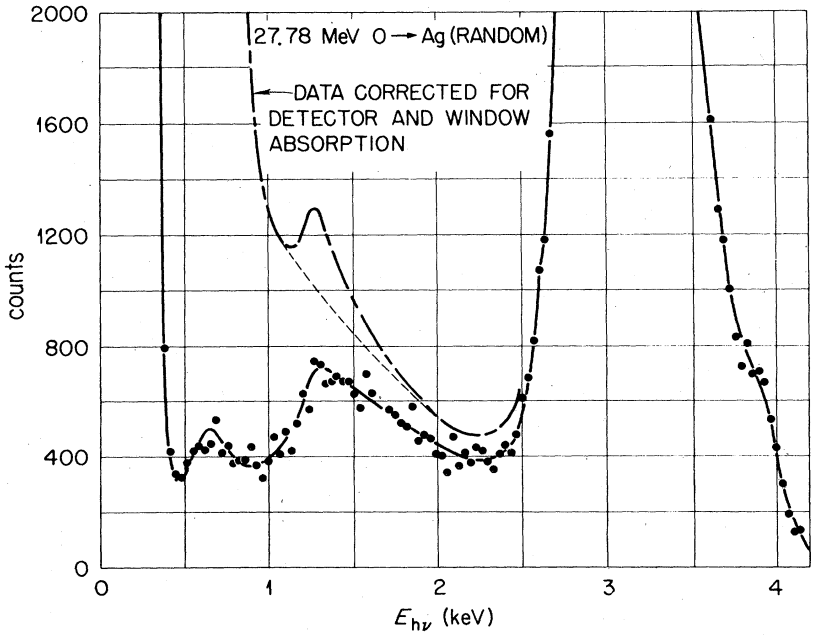

FIG. 6. Measured and absorption corrected photon spectra resulting from 27.78-MeV O transmitted through a 0.62-μm Ag single crystal in a random direction.

neling technique a useful simulation method for studying interactions relevant to this problem.[10]

B. Measurements on Ag

Measurements were made for oxygen ions of various selected charge states with energies from 17.8 to 40 MeV, transmitted parallel to the [001] and [011] axes, and (100) planes of Ag single crystals ranging in thickness from 0.40 to 0.80 μm. A typical channeling spectrum is shown in Fig. 7 before and after absorption corrections. The major interests from such spectra were the energies, widths, and areas of the REC peaks. The REC peaks were extracted by assuming background subtractions like those shown as light dashed curves. Although it mattered little whether corrected or uncorrected spectra were used, the REC results quoted were obtained from absorption-corrected spectra.

In addition to the REC features which are the major focus of this paper, it is clear from the rapidly rising portion of the spectrum below 1 keV in Fig. 7 that substantial contributions occurred from bremsstrahlung and/or x rays from O ions, as discussed in Sec. II C. Since the expected cut-off energy, $(m_e/M_1)E_1$, for beschleunigungsstrahlung coincides closely with the energy Z_1^2 Ry for series-limit O x rays, it is difficult to deduce from the data of Fig. 7 the relative contributions from these two mechanisms. It was possible to deduce qualitatively, however, from the results of a "beam-foil" type experiment shown in Fig. 8, and the Si measurements discussed in Sec. III C that both mechanisms were probably contributing. The two channeling spectra shown in Fig. 8 were obtained for 27.78-MeV O^{7+} ions incident parallel to the [011] and [001] axes, respectively, of a Ag single crystal. (Neither spectrum is corrected for absorption effects.) More significantly, however, because of the sample-detector geometry, when the crystal was tilted so that the beam was incident parallel to the [011] axes the Si(Li) detector had an unobstructed view of the crystal, but in the [001] orientation the Si(Li) could only see x rays originating outside the exit surface of the single crystal. No characteristic Ag L x rays or REC x rays are seen in the [001] spectrum, nor would one expect bremsstrahlung to originate outside the crystal, but a definite peak is seen just below 1 KeV. These are likely x rays emitted by highly excited O^{7+} ions which have lifetimes $\sim 10^{-12}$ sec.[31] Such x rays could originate either as a result of the incident O^{7+} ions being excited inside the crystals and de-exciting after emerging, or as O^{7+} ions which become O^{8+} ions inside the crystal, capture an electron to the continuum, and then decay to the ground state after leaving the single crystal. Although the first process would seem most likely, since O^{7+} ions are incident on the crystal, one must recall that measurements like those discussed in connection with Figs. 2 and 3 indicate that O^{7+} ions rapidly up-strip to O^{8+} in the channel. Experimental difficulties in the present experiments prevented a quantitative differentiation between the mechanisms of bremsstrahlung, excitation and de-excitation, and capture to the continuum, which might contribute to the x rays observed below 1 keV in the spectra of Fig. 8, but the channeling technique is a promising method for studying these phenomena in detail. Future experiments are planned in an ultrahigh vacuum environment using samples with well-characterized

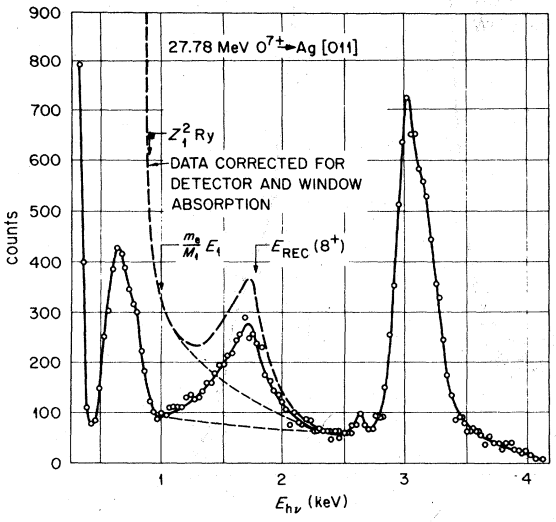

FIG. 7. Measured and absorption corrected photon spectrum resulting from 27.78-MeV O^{7+} ions transmitted parallel to the [011] axial channels of a thin Ag single crystal.

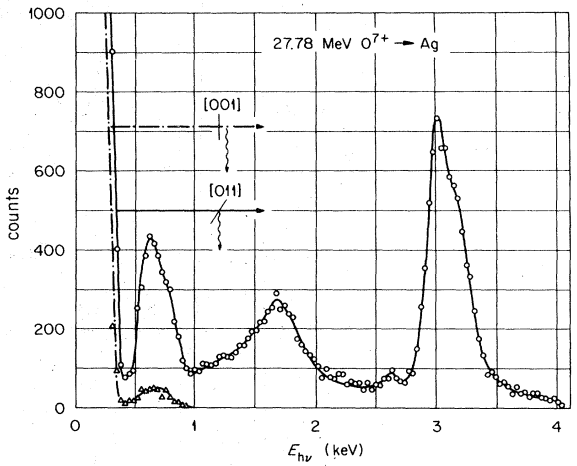

FIG. 8. Measured photon spectra resulting from oxygen ions transmitted parallel to the [001] and [011] axial directions of a thin Ag single crystal. See text for experimental conditions.

surfaces and a windowless Si(Li) detector and/or an x-ray crystal spectrometer.

C. Measurements on Si

Measurements on Si for O ions in the energy range 17.8–40 MeV were complicated because Si K x rays have an energy (1.74 keV) quite close to the REC x rays under investigation and because this energy range is near the maximum in the Si K excitation cross section. A sample spectrum is shown in Fig. 9 for 40-MeV O^{8+} ions incident in a random direction (solid circles) and parallel to the [011] axes (open circles) of a 2.8-μm-thick Si single crystal.[12] These spectra are normalized by the minimum yield fraction (i.e., the Si K peak intensities coincide) and they have not been corrected for absorption effects. At this energy the bremsstrahlung cut off $(m_e/M_1)E_1$ and the O-series limit (Z_1^2 Ry) are separated and there appears to be an excess of x rays in the channeling spectrum in this general region. Similarly an excess exists on the high-energy tail of the intense Si K peak which, when the channeling and random spectra are subtracted, might be interpreted as a radiative electron-capture peak (dashed curve). However, in both cases the evidence is much too tentative to draw any firm conclusions. If the REC feature were real it would signal a cross section considerably lower than observed for Ag.

A more meaningful series of measurements in Si would require O energies higher than those attainable with the present Tandem accelerator in order to separate further the REC peak from the Si K x rays. At such energies one can expect additional complications from beam initiated background radiation at defining aperatures and from nuclear reactions in the target.

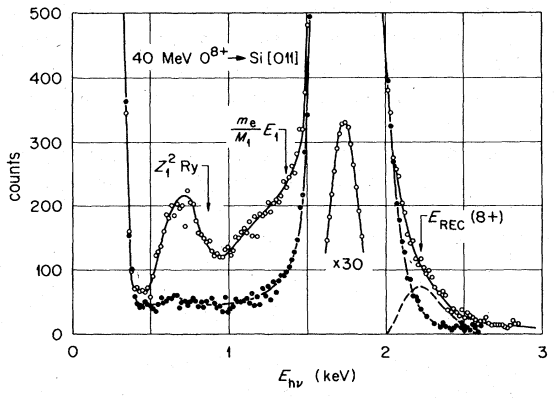

FIG. 9. Normalized photon spectra from 40-MeV O^{8+} ions transmitted parallel to [011] and in a random direction of a 2.8-μm Si single crystal.

IV. THEORY

Consider a solid through which a swift heavy ion of charge Z_1e and velocity $\vec{v}$ passes. Let $\vec{r}$ be the coordinate of a given one of the electrons in the solid relative to the ion and $\vec{R}$ be the coordinate of the center of mass of the ion and that electron. Capture of an electron accompanied by the emission of a single photon can occur. The nonrelativistic Hamiltonian of the system may be written $H = H_0 + H_{\rm rad} + H'$, where

$$H_0 = -\frac{1}{2}\frac{1+M}{M}\nabla_r^2 - \frac{1}{2(1+M)}\nabla_r^2 - \frac{Z_1}{r} \tag{1}$$

is the Hamiltonian of the electron-ion system,

$$H_{\rm rad} = \sum_{\vec{k}\lambda} \omega_k \left(a^\dagger_{\vec{k}\lambda} a_{\vec{k}\lambda} + \tfrac{1}{2}\right) \tag{2}$$

is that of the free radiation field and

$$H' = \sum_{\vec{k}\lambda} \left(\frac{2\pi}{\Omega\omega_k}\right)^{1/2} \hat{e}_{\vec{k}\lambda}\cdot\hat{O}\left(a^\dagger_{-\vec{k}\lambda} + a_{\vec{k}\lambda}\right) \tag{3}$$

is the interaction energy between them. A term in H' which is quadratic in the vector potential has been neglected. Atomic units ($\hbar = e = m = 1$) are used throughout this section. The mass of the ion is M, $a_{\vec{k}\lambda}$ is the annihilation operator of a photon with polarization index λ and wave vector $\vec{k}$, ω_k is the frequency of a photon of wave vector $\vec{k}$, and Ω is the normalization volume of the radiation field. The operator $\hat{O}$ is

$$\hat{O} = \exp\left[i\vec{k}\cdot\left(\vec{R} + \frac{M}{1+M}\vec{r}\right)\right]\left(\vec{P} + \frac{1}{1+M}\vec{p}\right) - \frac{Z_1}{M}\exp\left[i\vec{k}\cdot\left(\vec{R} - \frac{1}{1+M}\vec{r}\right)\right]\left(-\vec{P} + \frac{M}{1+M}\vec{p}\right) . \tag{4}$$

The first term in $\hat{O}$ represents the effect of electronic motion in coupling with the radiation field, while the second term originates in ionic motion. The momentum operators of relative and of center-of-mass motion are written $\vec{p}$ and $\vec{P}$, respectively.

In order to find an expression for the rate of photon emission accompanying capture of an electron into a bound state, the initial state vector, $|i\rangle$, is taken to be

$$|i\rangle = (1/\Omega^{1/2}) e^{i\vec{P}_0\cdot\vec{R}} u_0(\vec{r})|0\rangle . \tag{5}$$

The final state vector, $|f\rangle$, is written in the form

$$|f\rangle = (1/\Omega^{1/2}) e^{i\vec{P}_f\cdot\vec{R}} u_f(\vec{r}) a^\dagger_{k\lambda}|0\rangle . \tag{6}$$

$\vec{P}_0$ and $\vec{P}_f$ are the center-of-mass momenta in the initial and final states, respectively, and $|0\rangle$ is the vacuum state of the radiation field.

The probability of radiative capture μ per unit path length of the heavy ion may be written, in first-order perturbation theory,

$$\mu=\frac{2\pi}{v}\sum_i\sum_f\sum_{k\lambda}|\langle f|H'|i\rangle|^2\delta(E_i-E_f)\ , \qquad (7)$$

where sums over initial and final states of the electron-ion system, as well as sums over the momentum and polarization index of the photon, are indicated. If the dipole approximation is made in evaluating the matrix element $\langle f|H'|i\rangle$, only the term corresponding to electronic current contributes to μ. If one retains the lowest-order nonvanishing terms in the power series expansions of each of the exponentials entering Eq. (4), and uses the fact that $M\gg 1$, one finds

$$\langle f|H'|i\rangle\approx -i\left(\frac{2\pi}{\Omega\omega_k}\right)^{1/2}\delta^3(\vec{P}_0-\vec{P})\times\int d^3r\,u_f^*(\vec{r})\times\hat{e}_{\vec{k}\lambda}\cdot\left(\nabla_{\vec{r}}-\frac{Z_1\omega_k}{\epsilon_{0f}}\frac{\vec{v}}{c}\vec{k}\cdot\nabla_{\vec{r}}\right)u_0(\vec{r})\ , \qquad (8)$$

where $v=P_0/M$ is the initial ion velocity, and ϵ_{0f} is the energy corresponding to the specified electronic transition. In obtaining the second term in the large parenthesis of Eq. (8), the matrix element equivalence $(r)_{nm}=-(\nabla)_{nm}/\epsilon_{nm}$ has been used. At velocities v and photon energies of interest here the second term in Eq. (8), which originates in ionic motion, is $\lesssim 10\%$ of the first. It will be neglected in the remainder of this paper. Then we have

$$\mu=\frac{(2\pi)^2}{v\Omega}\sum_i\sum_{\vec{k}}\sum_\lambda\frac{1}{\omega_k}\left|\int d^3r\,u_f(\vec{r})\hat{e}_{\vec{k}\lambda}\cdot\nabla u_0(\vec{r})\right|^2\times\delta(\epsilon_i-\epsilon_f-\omega_k)\ , \qquad (9)$$

where the sum runs over initial states of relative motion, ϵ_i and ϵ_f are energies of relative motion in the initial and final states, respectively. Center-of-mass energies subtract in the argument of the energy-conserving delta function because of center-of-mass momentum conservation.

A rigorous evaluation of the matrix element in Eq. (9) would require a knowledge of the many-electron wave function of the solid through which the ion penetrates. In order to simplify the evaluation of μ we adopt a statistical approximation similar to that used successfully in computing energy loss of swift ions in matter[32] and in obtaining theoretical Compton x-ray profiles in solids.[33] This general approach involves the assumption that an infinitesimal element of volume in the solid at position $\vec{r}$ is characterized by the total electronic density $n(\vec{r})$ there, and that the response of this volume element is the same as that of an electron gas at the same density, independent of other parts of the solid. We employ fairly realistic $n(\vec{r})$ values which are computed from a relativistic Hartree-Fock program[34] using the Wigner-Seitz (WS) boundary condition.

Assume that the wave function of electrons in a given part of the solid may be represented in terms of momentum eigenfunctions. Then if $P_{0i}=Mv$ is the initial momentum of the ion and k_0 is that of an electron,

$$|i\rangle=\Omega^{-1}\exp(i\vec{P}_{0i}\cdot\vec{r}_i)\exp(i\vec{k}_0\cdot\vec{r}_e)=\Omega^{-1}\exp\left[i(\vec{P}_{0i}+\vec{k}_0)\cdot\vec{R}+\frac{i}{M+1}(M\vec{k}_0-\vec{P}_{0i})\cdot\vec{r}\right]\ , \qquad (10)$$

where $\vec{r}_i$ and $\vec{r}_e$ are the coordinates of the ion and electron, respectively. Then the initial energy of relative motion is

$$\epsilon_0=\frac{M+1}{2M}\left(\frac{\vec{P}_{0i}}{M+1}-\frac{M}{M+1}\vec{k}_0\right)^2\approx\tfrac{1}{2}(\vec{v}-\vec{k}_0)^2\ .$$

Taking

$$u_f(r)=(Z_1^3/\pi)^{1/2}\exp(-Z_1r)\ ,$$

corresponding to a K-shell orbital of the swift ion, one finds

$$\mu=\frac{8Z_1^5}{\pi^3v}\int d^3k_0\sum_\lambda\int\frac{d^3k}{\omega_0}\frac{(\hat{e}_{\vec{k}\lambda}\cdot\vec{p})^2}{(Z_1^2+p^2)^4}\times\delta(E_B+\tfrac{1}{2}p^2-\omega_k)\ , \qquad (11)$$

where $\omega_k=ck$, $E_B=\frac{1}{2}Z_1^2$ is the binding energy of an electron in the K orbital and $\vec{p}=\vec{k}_0-\vec{v}$. The integral over $\vec{k}_0$ covers a Fermi sphere of electrons. A factor of 2 for the possible spin states has been incorporated into Eq. (11). This result has been obtained by neglecting M^{-1} compared with unity throughout the development.

Transforming the integral over wave vector of the radiation field to an integral over photon energy ω_k and direction of emission $\hat{\Omega}_k$ by setting $d^3k=\omega_k^2d\omega_k d\hat{\Omega}_k/c^3$, one finds

$$\mu=\frac{(2Z_1)^5}{3\pi^2c^3}\int d^3k_0\frac{p^2}{(Z_1^2+p^2)^3}\ , \qquad (12)$$

where the sum over polarization index has been carried out. Integration may be carried out over directions of $\vec{k}_0$ referred to $\vec{v}$ as the z axis in a spherical polar system of coordinates. The integral over the magnitude of $\vec{k}_0$ may be transformed into an integral

over $\omega_k \equiv \epsilon$, the photon energy. After some algebra an expression is obtained for $d\mu/d\epsilon$, the differential inverse mean free path (DIMFP), for emission of a photon with energy ϵ per unit energy. The result is

$$\frac{d\mu}{d\epsilon} = \frac{16Z_1^5}{3\pi v^2 c^3}\left[\frac{\epsilon-\epsilon_B}{\epsilon^3}\{\epsilon_F - [(\epsilon_1)^{1/2} - (\epsilon-\epsilon_B)^{1/2}]^2\}\right] , \tag{13}$$

where ϵ_F is the Fermi energy, ϵ_B is the binding energy of the captured electron, and $\epsilon_1 = \frac{1}{2}v^2$ is the energy of an electron having the ion velocity. The large parenthesis in Eq. (13) should be set equal to zero unless we have

$$\epsilon_B + (\epsilon_1^{1/2} - \epsilon_F^{1/2})^2 < \epsilon < \epsilon_B + (\epsilon_1^{1/2} + \epsilon_F^{1/2})^2 . \tag{14}$$

ϵ must also be larger than ϵ_B. Equation (13) is taken as a central result in connection with the statistical approximation to the capture process. One may also use the Bethe-Salpeter cross section in deriving an expression for $d\mu/d\epsilon$. This is equivalent to assuming that each electron undergoing capture from the solid experiences the full Coulomb field of the projectile, and hence is in a continuum hydrogenic state of the bare ion before capture. Screening by other electrons of the solid may vitiate this assumption to some degree. One may show that use of Bethe-Salpeter cross section gives

$$\frac{d\mu_{BS}}{d\epsilon} = \frac{16Z_1^6}{3vc^3}\frac{f\left(\frac{\epsilon_B}{\epsilon-\epsilon_B}\right)}{\epsilon^2(\epsilon-\epsilon_B)} \times \{\epsilon_F - [(\epsilon_1)^{1/2} - (\epsilon-\epsilon_B)^{1/2}]^2\} , \tag{15}$$

where

$$f(x) = \frac{\exp[-4(x)^{1/2}\tan^{-1}(1/x^{1/2})]}{1-e^{-2\pi(x)^{1/2}}} , \tag{16}$$

and where the square bracket is understood again to be set equal to zero for values of ϵ not satisfying Eq. (14).

Relativistic Hartree-Fock-Slater calculations of $n(r)$, the electronic density in the WS sphere for a given solid, are available.[34] We assume that the local Fermi energy is $\epsilon_F(r) = \frac{1}{2}[3\pi^2 n(r)]^{2/3}$ when capture occurs from the vicinity of r in the Wigner-Seitz sphere. To account, approximately, for the fact that electrons at small r tend to be bound in the solid more strongly than those at larger values of r, the energy ϵ_B is decreased by an amount equal to a constant times the local Fermi energy ϵ_F, i.e., $\epsilon_B = \frac{1}{2}Z_1^2 - K\epsilon_F(r)$. The constant is $K \lesssim 1$ and may be chosen to fit the experimental data.

In order to obtain a distribution of photon energies appropriate to all trajectories of an ion in a given channeling state the simplifying assumption is made that the ion samples, on straight-line trajectories, all portions of the WS sphere corresponding to impact parameters b greater than $b_{\min}$. This minimum value $b_{\min}$, in general, depends on v, Z_1, and the lattice potentials. On this model the average of the DIMFP over straight trajectories for the case of axial channeling may be written

$$\left\langle\frac{d\mu}{d\epsilon}\right\rangle = \frac{3}{2r_{WS}^3}\int_{b_{\min}}^{r_{WS}} x\,dx \int_{-(r_{WS}^2-x^2)^{1/2}}^{(r_{WS}^2-x^2)^{1/2}} dy\,\frac{d\mu(r)}{d\epsilon} , \tag{17}$$

where $r^2 = x^2 + y^2$. Transforming to spherical polar coordinates one finds

$$\left\langle\frac{d\mu}{d\epsilon}\right\rangle = \frac{3}{r_{WS}^3}\int_{b_{\min}}^{r_{WS}} r(r^2-b_{\min}^2)^{1/2}\frac{d\mu}{d\epsilon}[\epsilon_F(r)]\,dr . \tag{18}$$

Then the distribution of emitted photons is taken to be

$$\left\langle\frac{d\mu}{d\epsilon}(\epsilon)\right\rangle = \frac{16}{\pi r_{WS}^3}\frac{Z_1^5}{v^2c^3}\int_{b_{\min}}^{r_{WS}} r(r^2-b_{\min}^2)^{1/2}\left[\frac{\epsilon-\epsilon_B(r)}{\epsilon^3}(\epsilon_F(r) - \{(\epsilon_1)^{1/2} - [\epsilon-\epsilon_B(r)]^{1/2}\}^2)\right]dr . \tag{19}$$

Use of the Bethe-Salpeter cross section gives the alternative expression

$$\left\langle\frac{d\mu_{BS}}{d\epsilon}\right\rangle = \frac{16Z_1^6}{r_{WS}^3c^3v}\int_{b_{\min}}^{r_{WS}}\frac{r(r^2-b_{\min}^2)^{1/2}}{\epsilon^2[\epsilon-\epsilon_B(r)]}f\left(\frac{\epsilon_B}{\epsilon-\epsilon_B}\right)\{\epsilon_p - [(\epsilon_1)^{1/2} - (\epsilon-\epsilon_B)^{1/2}]^2\}\,dr . \tag{20}$$

In the present applications, Eqs. (19) and (20) predict essentially the same dependence of DIMFP and IMFP on projectile velocity and differ in magnitude only slightly. The value of $b_{\min}$ appropriate to a given experiment, may be taken from theory. In the present application this schematic distribution of impact parameters will suffice to demonstrate the usefulness of this model. Further work could employ more accurate information about the impact parameter distribution.

As discussed above, two sources of bremsstrahlung should contribute importantly to the measurements

described here. The distribution of photons originating from the direct acceleration of target electrons in the Coulomb field of the swift ion (beschleunigungsstrahlung) may be estimated by assuming that the struck electrons are free and at rest. Using the Bethe-Salpeter result[28] for the differential bremsstrahlung cross section at nonrelativistic energies, one finds

$$\frac{d\mu_{DB}}{d\epsilon} \cong \frac{16}{3}\frac{\langle n\rangle Z_1^2}{c^3 v^2 \epsilon}\ln\left[\frac{v+(v^2-2\epsilon)^{1/2}}{v-(v^2-2\epsilon)^{1/2}}\right](\text{Å}) \qquad (21)$$

for the DIMFP for emission of a photon of energy ϵ, if the ion velocity is v. All quantities entering Eq. (17) are expressed in atomic units, and $\langle n\rangle$ is the mean density of electrons seen by the ion.

The distribution of photons generated in collisions of knock-on electrons with lattice ions should be computed accounting for the buildup of electron flux in the energy degradation process. An ion of charge Z_1 moving in a uniform solid in which the electron density is (constant at) n_0, gives rise to a spectrum of knock-on electrons described by

$$\frac{d\lambda_K^{-1}}{dT} = \frac{2\pi n_0 Z_1^2}{v^2}\frac{1}{T^2}\Theta(T_{\max}-T)\ , \qquad (22)$$

where $d\lambda_K^{-1}/dT$ is the differential probability per unit length of ion travel for generation of an electron with kinetic energy T per unit energy interval. Struck electrons are assumed initially at rest. $T_{\max}$, appearing in the argument of the Heaviside step function $\Theta(x)$, is equal to $2mv^2$ (in ordinary units) and is the maximum energy in the knock-on distribution. We may approximate the degradation spectrum created in the solid by knock-on electrons from[35]

$$\frac{d\phi}{dT} = \frac{1}{S(T)}\int_T^{T_{\max}}\frac{d\lambda_K^{-1}}{dT'}dT' = \frac{2\pi n_0 Z_1^2}{v^2 S(T)}\left[\frac{1}{T}-\frac{1}{T_{\max}}\right]\text{a.u.}\ , \qquad (23)$$

where $d\phi/dT$ is the probability of finding an electron with energy T anywhere in the solid per unit energy interval, and $S(T)$ is the stopping power of the solid for electrons with energy ϵ. Note that this will tend to overestimate the distribution since it is derived neglecting, (i) loss of electrons through the surfaces of the foil and (ii) binding of struck electrons. Electrons at each energy in the distribution Eq. (19) may generate bremsstrahlung photons in scattering on lattice atoms. The number of photons with energy ϵ resulting will be given by the convolution of Eq. (21) and Eq. (23), where in Eq. (23) we set $n_0 = \langle n\rangle$ in Eq. (21) we set $\langle n\rangle Z_1^2 \rightarrow n_A Z_A^2$, where n_A is the nuclear density in the solid and Z_A is the charge on the nucleus.[36] Thus the number of photons with energy ϵ produced per unit path length of the ion, may be computed from

$$\frac{d\mu_K}{d\epsilon} = \frac{16\pi}{3}\frac{\langle n\rangle n_A Z_1^2 Z_A^2}{v^2 c^3 \epsilon}\int_\epsilon^{T_{\max}}\frac{dT}{T}\left[\frac{1}{T}-\frac{1}{T_{\max}}\right]\frac{1}{S(T)}\ln\left[\frac{T^{1/2}+(T-\epsilon)^{1/2}}{T^{1/2}-(T-\epsilon)^{1/2}}\right] \qquad (24)$$

As discussed above in Sec. III C there are many solid-state effects, as well as "atomic" effects which may contribute to the continuum background of x-rays in these experiments. Hence an absolute comparison of the predictions of Eqs. (19), (20), and (24) with experiment is not feasible. We show below, however, that normalization of the experimental REC peak to theory using Eqs. (19) or (20) brings the background continuum of x rays into reasonable agreement with the results for bremsstrahlung from knock-ons as computed from Eq. (24).

V. RESULTS

A. REC peak energy dependence

The energetics of the REC process indicate that the REC peak energy should vary with incident ion energy E_1 and charge Z_1 as $E_{\text{REC}} = (m_e/M_1)E_1 + Z_1^2$ Ry. Results for a variety of measurements using O^{6+}, O^{7+}, and O^{8+} ions in [011], (100), and random directions of Ag single crystals, and in Si[011] are summarized in Fig. 10. The two solid lines on the figure are the calculated REC energies assuming capture

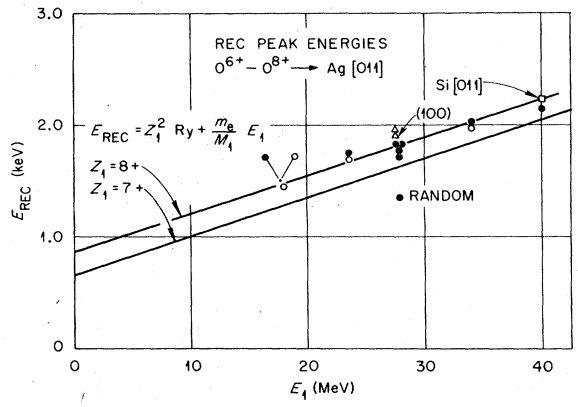

FIG. 10. Measured REC peak energies versus incident ion energies compared to calculations.

into a 7+ or 8+ ion as noted. The data points are not labeled according to incident charge state since no systematic variation could be detected. It appears from Fig. 10 that, excepting the random value, the measured REC peak energies agreed most nearly with the energies expected for capture into a fully stripped O^{8+} ion regardless of input charge state. This observation is consistent with earlier charge-state measurements for channeled O ions which show that the ions rapidly up-strip to O^{8+} in a single-crystal channel.[16–19]

B. REC line shapes and bremsstrahlung

Figure 11 shows comparisons between measurements of a typical distribution of photon energies in a REC peak, and calculations of the REC distribution from Eq. (19).[37] A smoothed background was subtracted from the experimental points after correction for window absorption and the distribution was normalized to the theoretical curve at a photon energy of 67 a.u. Also shown in this figure is the experimental x-ray distribution remaining after the REC peak is subtracted, shown as a dot-dashed line. For comparison the bremsstrahlung yield from knock-on electrons computed from Eq. (24) is shown as a dashed line.[38]

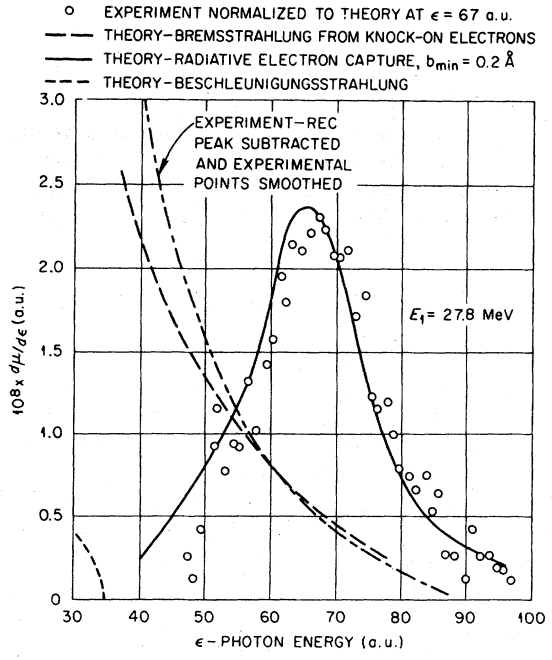

FIG. 11. Comparison of measured REC peak and subtracted background to theoretical calculations described in the text. The pertinent theoretical parameters are shown on the figure.

The agreement is quite good considering the uncertainties in the theoretical model and the possibility of contributions from other solid-state processes (see Sec. II C). We also indicate the small contribution expected from the beschleunigungsstrahlung process (the short-dashed curve) in which electrons of the solid are accelerated by the projectile and emit radiation in the process (see Sec. II C).

C. REC cross sections

It is also possible to extract REC cross sections and line widths from the measurements. The yield of REC relative to Ag L x rays for a channeling situation can be obtained from the areas under the respective peaks in a corrected spectrum such as Fig. 7. When the Ag target is in a random orientation, the area under the Ag L x-ray peak can be related to measurements of the absolute Ag L cross sections which have been made in separate experiments.[39] In going from a random to a channeling target configuration, the Ag L-x-ray yield is reduced by the minimum yield fraction as a result of the channeling effect. The minimum yield can be accurately measured using the beam monitoring arrangement. Thus by comparing the areas of the REC and Ag L-x-ray peaks in the channeling spectrum, and relating these to the random spectrum and absolute cross-section measurements through the minimum yield it is possible to obtain cross sections for REC. Note that, to conform with practice in this area, the cross sections given are in cm^2 per atom of Ag in the solid. The theoretical differential inverse mean free paths computed as described in Sec. IV have been divided by the atomic density of Ag in order to compare with experimentally derived cross sections.

Results from our measurements on Ag and Si are compared in Fig. 12 to measurements by Schnopper *et al.*[5] for REC by oxygen ions in N_2 and O_2 gases and to theoretical calculations. Consider first the left-hand side of Fig. 12. The symbols in the upper portion of the figure are marked with the incident ion charge state and represent our measured results. A line is drawn through the data points for cognizance. One can see that there does not appear to be a strong input charge-state effect. Measured REC cross sections for planar channeling (100), appear to be lower than axial results at the same energy, and the one Si point appears considerably lower than the comparable Ag result. The Si measurement is, however, somewhat speculative because of the difficulty in extracting the REC peak from the tail of an intense Si K-x-ray line. The data corrections for absorption which are applied are listed on the left-hand side portion of the figure.

Now consider the right-hand half of Fig. 12. The curved solid line in the upper portion of the figure is

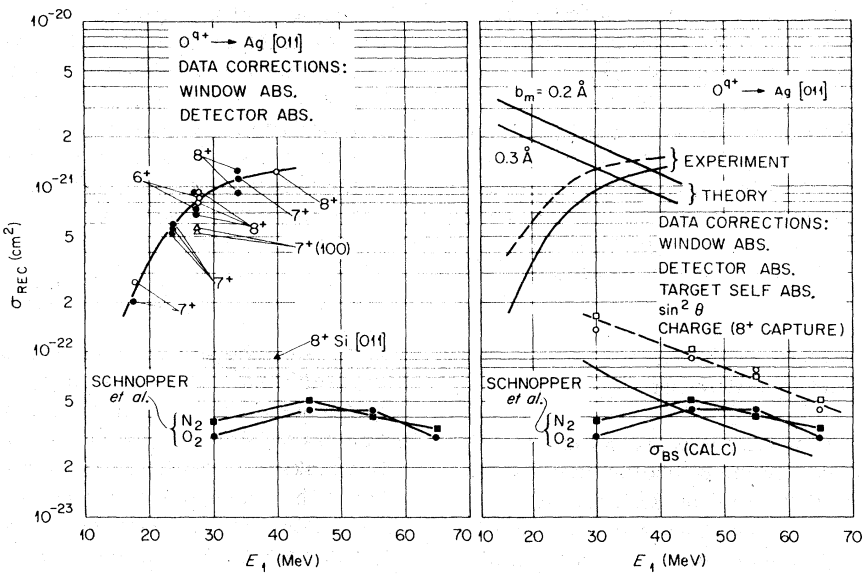

FIG. 12. Corrected REC cross sections measured for various incident charge states, energies and targets, and compared to the theoretical calculations in the text.

simply the line drawn through the data points in the left-hand half of the figure transferred to the right-hand side for comparison. The dashed curve above this line shows the effects of correcting the data for target self-absorption, for the angular dependence of the REC effect, and a charge-state correction. The charge-state correction was made on the assumption that only the fraction of oxygen ions which are initially 8+ inside the single-crystal channel contribute substantially to the observed REC effect. This charge-state correction was also applied to the data of Schnopper *et al.* (lower portion of right-hand side) and the results are shown as the dashed line above this data. The correction is actually more straight forward for the gas measurements of Schnopper *et al.* than for our case because the charge-state distributions for oxygen ions in gases are well known and unambiguous. As discussions in Secs. I–IV have shown, the actual charge-state distribution for channeled oxygen ions *inside* the single-crystal solid are difficult to know. The charge-state distribution which we used in our correction procedure are deduced from measurements such as those represented in Fig. 2, which indicate the charge fractions of *emerging* ions. Measurements like those corresponding to Fig. 3 indicate that a substantial portion of this charge exchange can occur at the entrance and exit surfaces of the crystal. Consequently, the charge-state corrections applied to our results are somewhat artificial and are likely to make the REC cross section appear larger than it really is. The rationale for estimating the charge-state correction was to see if this could account for the discrepancy between measurement and theory evident from Fig. 12. Furthermore, theoretical calculations[1,7] indicate that free electrons are most likely captured into the innermost shell, and O^{8+} capture is more probable than O^{7+} capture because of the density-of-states agrument. There is also experimental evidence such as that argued in Secs. I–IV that the ions are largely 8+ in the channel regardless of input charge.

The lines labeled *Theory* in Fig. 12 were calculated by integrating Eq. (18) numerically over photon energy for two different values of $b_{\min}$, 0.2 and 0.3 Å. In order to convert the inverse mean free paths so obtained to a cross section per Ag atom, we have divided by the atomic density of the solid. Although the theory agrees reasonably well in magnitude with experiment, the energy dependences are quite different.

D. REC line widths

Radiative electron capture line widths extracted from measurements such as those in Fig. 7 and corrected for detector resolution are shown in Fig. 13 as solid bars. Measurements were made using ions with various input charge states and energies, with crystals of various thickness, and using several different Si(Li) detectors with both 0.0003-in. and 0.0005-in. Be windows. The vertical extent of the bars encompasses all such effects at each incident energy. The solid line labelled Theory shows line widths calculated from the distributions described by Eq. (18) for $b_{\min}=0.2$ and 0.3 Å for REC by O^{8+} ions channeled in Ag single-crystal channels.[32] The dashed line was taken from a free-electron model calculation by Schnopper *et al.*[5]

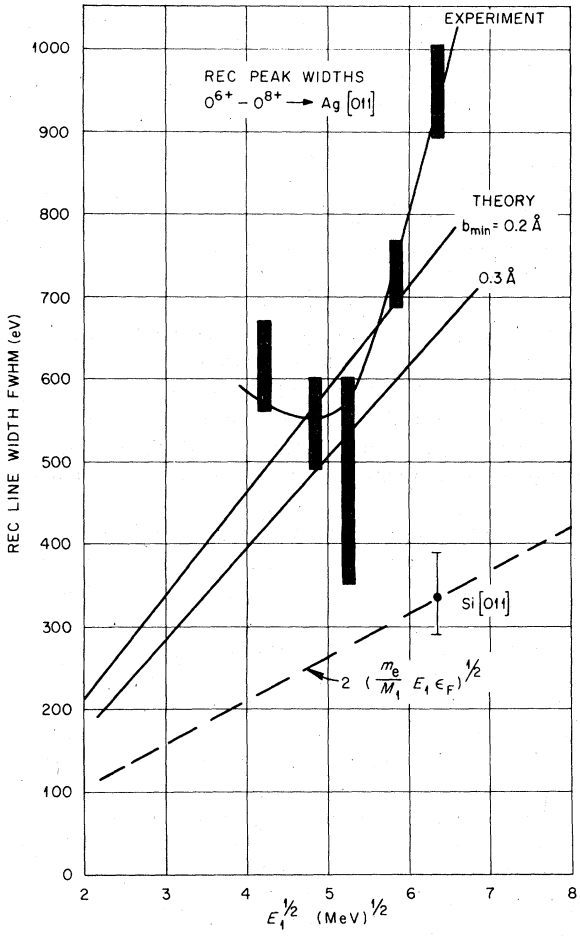

FIG. 13. Measured REC line widths compared to theoretical calculations.

VI. DISCUSSION OF RESULTS

There are both encouraging and perplexing aspects to the results obtained in the present investigation. The functional dependence of our measured REC cross sections on ion energy, Fig. 12, are not in good agreement with either the calculations based on the Bethe-Salpeter method[1] or the more pertinent calculations detailed in Sec. IV. The phenomena of electron capture in general are not well understood. Only the simplest cases for nonradiative capture of bound electrons by hydrogen and helium ions have been treated.[7] There are essentially no treatments applicable to bound electron capture for heavy ions, particularly for partially stripped heavy ions. Radiative electron capture is, by comparison, based on a more reliable framework if one accepts the Bethe-Salpeter approach to the problem. Furthermore, our experimental technique should, as we have already discussed, be particularly amenable to the Bethe-Salpeter approach since we are dealing with a hydrogen-like ion (O^{8+}) in a free-electron gas (conduction electrons). We, therefore, would expect much better agreement than we have achieved.

It is also instructive to consider the behavior of other experimental results. As Fig. 12 shows, the results of Schnopper *et al.*[5] for REC by oxygen ions in N_2 and O_2 gases are in quite good agreement with calculations based on a free-electron theory once they are corrected for charge-state effects. In this case the oxygen ions are mostly 8+ at the higher energies so the charge-state corrections are, in general, small. The measurements are, however, in gaseous targets. Lindskog *et al.*[8] measured REC for 9 to 58 MeV chlorine ions in thin polycrystalline foils of carbon and nickel. In this case the chlorine ions had a distribution of charge states from 7+ to 13+ which complicate the interpretation as discussed in earlier parts of this paper. Furthermore, competition between characteristic $K\alpha$ and $K\beta$ x-ray transitions and the REC process, requires assumptions concerning the radiative decay rates for the K vacancy and complicates interpretation somewhat. Nevertheless, Lindskog *et al.*[8] report good agreement between measured REC cross sections in the carbon foils and calculations using the Bethe-Salpeter theory; but they reported quite anomalous results for the nickel foils.

Recently Koyama and Ohtsuki[40] reported calculations of REC based on a model which accounted for the electronic structure of the metal surface, and Úlehla and Davis reported corrected REC calculations utilizing this same model.[41] These calculations are stimulating in that they include the surface features of the metal, but it is doubtful that surface REC plays a significant role in the results reported here. The electron-capture effects observed in measurements of energy-loss spectra as a function of charge-state, like those discussed in connection with Fig. 3, are probably nonradiative capture events which occur in the few monolayers of contaminants on the Ag crystal surfaces. These effects may alter REC by altering the charge-state population of the channeled beam but are not related to the surface-capture phenomenon calculated in the above papers. Nevertheless, it is possible that some solid-state effect may prove instrumental in explaining our measurements.

As Fig. 11 shows, the shape of the measured REC lines can show good agreement with REC distributions calculated from Eq. (19). Furthermore, the remaining x-ray background is in reasonable agreement with calculations of the bremsstrahlung yield from knock-on electrons computed from Eq. (24). These results are encouraging since they indicate that REC experiments in the channeling configuration may be a viable tool for determining the velocity distributions of electrons in single-crystal channels. On the other hand, the measured widths of REC lines

obtained from many measurements at various ion energies, Fig. 13, show only fair agreement with calculations. Widths extracted at the same incident ion energy and crystal orientation but for different crystals, input charge states, and experiments show an unusually large variation, and the general trend of the curve is not well reproduced. The reasons for this scatter are under investigation. The differences may be related to varying surface conditions on the Ag crystals from experiment to experiment or differing absorption characteristics from one Si(Li)-detector–Be-window combination to another.

At present we do not have a quantitative explanation for the major disagreement between the energy dependence of our measured REC cross sections and the calculations. The theory on REC presented here does not account for some effects due to the dynamic interaction between the ion and the solid. For example, collision broadening of the energy of an electron captured in the K shell of the projectile should tend to make the distribution of photons wider than calculated above; this effect may become more important as the projectile velocity decreases and as impact parameter relative to strings of atoms in the solid decreases. The time-varying potential of the lattice seen at the position of the ion may contain Fourier components which coincide with important transition frequencies of an electron from the K shell of the ion.[42] In this case, the probability of capture of an electron into this shell could be affected appreciably. In addition, at small impact parameters the binding energy of a K electron to the projectile must be affected by its proximity to a string. The presence of a wake of density fluctuations[43] trailing the projectile is also expected to affect the binding. The present theoretical state of art does not permit one to make accurate estimates of the effect of these mechanisms of REC probability. It is conceivable, however, that these phenomena might account for the trend of the experimental REC IMFP with increasing energy (Fig. 12).

The primary interest of this work was to utilize the unique constraints of the channeling technique to investigate the REC effect under well-defined conditions, and to provide a theoretical interpretation specifically modified to include these constraints. The measurement technique itself shows great promise. Our measurements indicate that it is possible to prepare a beam of 40-MeV O^{8+} ions which, when channeled, remains in the 8+ charge state and interacts with the atoms of the solid at large impact parameters only. Consequently, this technique should be a valuable tool for extracting the velocity distributions of electrons along various crystallographic directions in single-crystalline solids. In order to exploit this capability to the fullest, one needs to do high-resolution experiments on single crystals with well-characterized surfaces, in ultrahigh vacuums, so as to eliminate or understand the surface capture effects observed in the present experiments. The generally good agreement between the calculated and measured REC line shapes which we see is a further encouraging indication. Similarly, many of the other effects contributing to the observed x-ray spectra (Sec. II C) can be manipulated by the channeling effect and studied under unique circumstances. On the other hand, the major disagreement between the energy dependence of our measured REC cross sections and the calculations is disturbing. The measurement technique employing the channeling effect should have improved the applicability of the calculations instead of complicating them. It is possible that channeling effects are responsible for contributing or enhancing some competing mechanism or solid-state effect. At the present time, we do not have a suitable explanation for the observed discrepancies but rely on future investigations to reveal their origins.

ACKNOWLEDGMENTS

The authors are grateful for helpful conversations with Werner Brandt and J. H. Barrett. We appreciate discussions with H. L. Davis, M. K. V. Ulehla, and Y. H. Ohtsuki concerning their REC calculations prior to publication. The technical expertise of the Tandem Accelerator staff is gratefully acknowledged. Research sponsored by the Division of Materials Sciences, U. S. DOE under Contract No. W-7405-eng-26 with the Union Carbide Corporation.

*Max-Planck-Institut für Plasmaphysik, 8046 Garching, West Germany.

†Subsequently at Bhabha Atomic Research Centre, Bombay, India. Now deceased.

[1]H. A. Bethe and E. E. Salpeter, *Quantum Mechanics of One- and Two-Electron Atoms* (Academic, New York, 1957), p. 320.

[2]H. W. Schnopper, H. D. Betz, J. P. Delvaille, K. Kalata, A. R. Sohval, K. W. Jones, and H. E. Wegner, Phys. Rev. Lett. 29, 898 (1972).

[3]P. Kienle, M. Kleber, B. Povh, R. M. Diamond, F. S. Stevens, E. Grosse, M. R. Maier, and D. Proctel, Phys. Rev. Lett. 31, 1099 (1973).

[4]H. W. Schnopper, J. P. Delvaille, K. Kalata, A. R. Sohval, M. Abdulwahab, K. W. Jones, and H. E. Wegner, Phys. Rev. Lett. 47, 61 (1974).

[5]H. W. Schnopper and J. P. Delvaille, in *Atomic Collisions in Solids*, edited by S. Datz, B. R. Appleton, and C. D. Moak (Plenum, New York, 1975), Vol. II, p. 481.

[6]B. R. Appleton, T. S. Noggle, C. D. Moak, J. A. Bigger-

staff, S. Datz, H. F. Krause, and M. D. Brown, *ibid.*, Ref. 5, p. 499.
[7]H. D. Betz, Rev. Mod. Phys. 44, 465 (1972).
[8]J. Lindskog, J. Pihl, R. Sjödin, A. Marelius, K. Sharma, R. Hallin, and P. Lindner, Uppsala University Institute of Physics Report UUIP-928, SW ISSN 0-042-0263, April (1976) (unpublished).
[9]H. D. Betz, in Proceedings of Heavy-Ion Summer Study, Oak Ridge, Tenn., edited by S. T. Thornton, ORNL Report No. CONF-720669, 1972 (unpublished).
[10]B. R. Appleton, R. H. Ritchie, J. A. Biggerstaff, T. S. Noggle, S. Datz, C. D. Moak, and H. Verbeek, J. Nucl. Mater. 63, 513 (1976).
[11]J. S. Briggs and K. Dettman, Phys. Rev. Lett. 33, 1123 (1974).
[12]We are indebted to R. L. Meek of Bell Laboratories for providing us with the Si single crystal; R. L. Meek, W. M. Gibson, and R. H. Braun, Nucl. Instrum. Meth. 94, 435 (1971).
[13]D. S. Gemmell, Rev. Mod. Phys. 46, 129 (1974).
[14]B. R. Appleton, S. Datz, C. D. Moak, and M. T. Robinson, Phys. Rev. B 4, 1452 (1971), and references therein.
[15]M. T. Robinson, Phys. Rev. B 4, 1461 (1971).
[16]F. W. Martin, Phys. Rev. Lett. 22, 329 (1969).
[17]S. Datz, F. W. Martin, C. D. Moak, B. R. Appleton, and L. B. Bridwell, Radiat. Eff. 12, 163 (1972).
[18]C. D. Moak, S. Datz, B. R. Appleton, J. A. Biggerstaff, M. D. Brown, H. F. Krause, and T. S. Noggle, Phys. Rev. B 10, 2681 (1974).
[19]Unreported data for hyperchanneling of oxygen ions by the method described in B. R. Appleton, C. D. Moak, T. S. Noggle, and J. H. Barrett, Phys. Rev. Lett. 28, 1307 (1972); and B. R. Appleton, J. H. Barrett, T. S. Noggle, and C. D. Moak, Radiat. Eff. 13, 171 (1972).
[20]J. D. Garcia, R. J. Fortner, and T. M. Kavanagh, Rev. Mod. Phys. 45, 111 (1973).
[21]D. H. Madison and E. Merzbacher, in *Atomic Inner-Shell Processes*, edited by B. Crasemann (Academic, New York, 1975).
[22]F. Folkmann, in *Proceedings of the Second International Conference on Ion Beam Surface Layer Analysis*, edited by O. Meyer, G. Linker, and F. Käppeler (Plenum, New York, 1975), Vol. II, p. 695.
[23]J. R. Mowat, I. A. Sellin, D. J. Pett, R. S. Peterson, M. D. Brown, and J. R. MacDonald, Phys. Rev. Lett. 30, 289 (1973); J. R. Mowat, I. Sellin, P. M. Griffin, D. J. Pett, and R. S. Peterson, Phys. Rev. A 9, 644 (1974); and S. J. Czuchlervski, J. R. MacDonald, and C. D. Ellsworth, Phys. Rev. A 11, 1108 (1975).
[24]D. Burch, N. Stolterfoht, D. Schneider, H. Wieman, and J. S. Risley, Phys. Rev. Lett. 32, 1151 (1974).
[25]D. K. Olsen, C. F. Moore, and P. Richard, Phys. Rev. A 7, 1244 (1973); and D. K. Olsen and C. F. Moore, Phys. Rev. Lett. 33, 194 (1974).
[26]F. W. Saris, W. F. Van der Weg, H. Tawara, and R. Laubert, Phys. Rev. Lett. 28, 717 (1972); H. D. Betz, F. Bell, H. Panke, W. Stehling, E. Spindler, and M. Kleber, Phys. Rev. Lett. 34, 1256 (1975); and C. K. Davis and J. S. Greenberg, Phys. Rev. Lett. 32, 1215 (1974).
[27]F. W. Saris, in *Atomic Collisions in Solids*, edited by S. Datz, B. R. Appleton, and C. D. Moak (Plenum, New York, 1975), Vol. I, p. 343.
[28]H. A. Bethe and W. Heitler, Proc. R. Soc. Lond. A 146, 83 (1934).
[29]C. W. Nestor, T. C. Tucker, T. A. Carlson, L. D. Roberts, F. B. Malik, and C. Froese, ORNL Report No. 4037, Clearinghouse for Federal Scientific and Technical Info., NBS, U. S. Dept. of Commerce, Springfield, VA 22151.
[30]F. Folkmann, C. Gaarde, T. Huus, and K. Kemp, Nucl. Instrum. Meth. 116, 487 (1974).
[31]*Atomic Transition Probabilities*, edited by W. L. Wiese, M. W. Smith, and B. M. Glennon (NBS, Ref. Data Series, U.S. Dept. of Commerce, NSROS-NBS4, 1965), Vol. I, p. 112.
[32]J. Lindhard, M. Scharff, and H. E. Schiøtt, K. Dan. Vidensk. Selsk. Mat.-Fys. Medd. 33, 14 (1963); E. Bonderup, *ibid.*, 35, 17 (1967).
[33]L. Lam and P. M. Platzman, Phys. Rev. B 9, 5122 (1974); *ibid.*, 9, 5128 (1974).
[34]See, e.g., T. C. Tucker, L. D. Roberts, C. W. Nestor, Jr., T. A. Carlson, and F. B. Malik, Phys. Rev. 178, 998 (1969).
[35]L. V. Spencer and F. H. Attix, Rad. Research 3, 239 (1955).
[36]Screening of the nuclei by electrons in the solid modifies somewhat the distribution obtained from Eq. (17) at low photon energies [see the qualitative description by J. D. Jackson, *Classical Electrodynamics* (Wiley, New York, 1962), Chap. 15]. At energies of interest here such screening is not important.
[37]The authors are grateful for the assistance of C. W. Nestor, Jr., who kindly supplied us with results of calculations of electron density in the Ag Wigner-Seitz cell.
[38]The stopping power of aluminum metal for these relatively-low-energy knock-on electrons has been taken from the work of J. C. Ashley, C. J. Tung, and R. H. Ritchie, Surf. Sci. (to be published).
[39]G. Bissinger, P. H. Nettles, S. M. Shafroth, and A. W. Waltner, Phys. Rev. A 10, 1932 (1974).
[40]K. Koyama and Y. H. Ohtsuki, Phys. Rev. B 15, 61 (1977).
[41]M. K. V. Úlehla and H. L. Davis, Phys. Rev. B 16, 4185 (1977).
[42]C. D. Moak, S. Datz, O. H. Crawford, H. F. Krause, P. F. Dittner, J. Gomez del Campo, J. A. Biggerstaff, P. D. Miller, P. Hvelplund, and H. Knudsen, Phys. Rev. Lett. (to be published).
[43]R. H. Ritchie, P. M. Echenique, and W. Brandt, Phys. Rev. B 14, 4808 (1976).